# Alpha-particle losses due to resonant magnetic perturbations and error fields in STEP

**F. Camilo de Souza**[1], **K. McClements**[1], **G. Xia**[1], **J. Morris**[1], **S. Bakes**[1]

[1]United Kingdom Atomic Energy Authority, UKAEA, Culham Campus Abingdon OX14 3DB UK

E-mail: fabio.camilo.de.souza@ukaea.uk

## 1. Introduction

### *1.1. STEP – Spherical Tokamak for Energy Production*

STEP is a UK-led programme to develop a tokamak fusion power plant prototype producing approximately 1.5 GW of fusion power, of which fusion alpha particles carry around 300 MW. Confinement of these alpha particles is critical to provide self-heating required to sustain a burning plasma avoid energy deposition on plasma-facing components.

The D-T fusion reactivity becomes appreciable at temperatures of approximately 7 keV and increases rapidly above 10 keV. In STEP, these temperatures are reached relatively close to the plasma edge ($\psi_N \sim 0.6$), exposing alpha particles to edge perturbations. Figure 1 shows the plasma equilibrium and alpha-particle birth profiles for a STEP scenario.

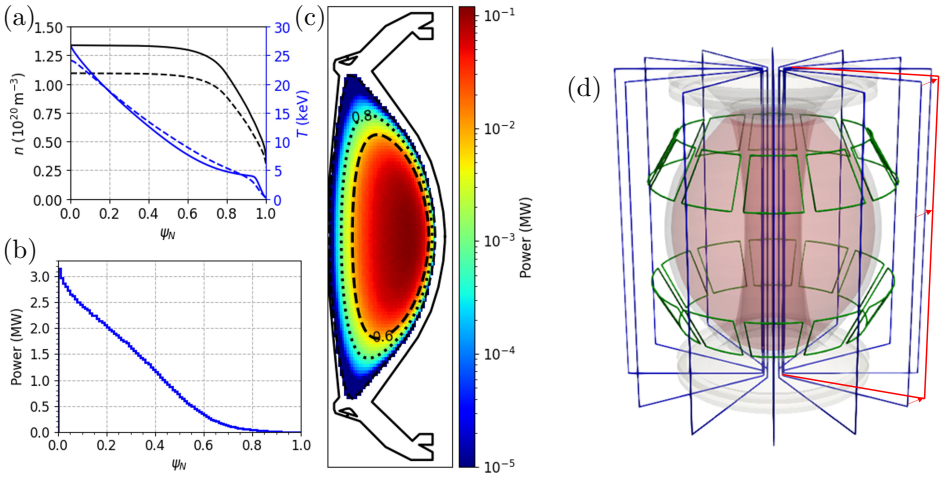


Figure 1: (a) Electron (solid) and ion (dashed) temperature profiles. (b) Fusion alpha-power generation as a function of normalized poloidal flux. (c) Fusion alpha-power distribution in the R–Z plane. (d) TF coils in blue, with a misaligned coil in red. RMP coils in green.

The STEP PFCs are replaceable, but acceptable lifetimes must be demonstrated. Minimising alpha-particle losses also reduces impurities sputtering from PFCs. The divertor can withstand heat fluxes up to 20 MWm$^{-2}$. The first wall limit is 2 MWm$^{-2}$, while radiation and other sources accounts for $\sim$ 1.5 MWm$^{-2}$, hence the allowable alpha-particle heat flux is 0.5 MWm$^{-2}$. Since the axisymmetric PFC model is expected to underestimate local loads, a conservative limit of 0.2 MWm$^{-2}$ is adopted.

Fast ions are highly sensitive to three-dimensional (3D) magnetic field perturbations [1, 2]. These perturbations break the conservation of toroidal canonical momentum, leading to enhanced transport and first-wall heat loads.

Toroidal field (TF) ripple arises from the finite number of TF coils (12 in STEP). In addition, thermal and mechanical loading during operation can displace the TF coils, the expected maximum is up to $\Delta_{\text{error}} \sim 3$ cm. These misalignments break the periodic symmetry of the ripple field, redistributing heat loads and introducing a new source of transport. Resonant magnetic perturbations (RMPs) provide an effective method for edge-localized mode (ELM) control. STEP current design includes two sets of 12 RMP coils for ELM mitigation scenarios. Figure 1 d) shows the TF and RMP coils.

The plasma response to the RMPs can shield the core from edge perturbations, but it potentially introduces new transport channels that degrade fast-ion confinement [3]. Plasma screening is generally stronger in low-resistivity, rapidly rotating plasmas, whereas the perturbation in highly resistive and slowly rotating plasmas approach the vacuum-field limit. STEP plasmas are expected to have only modest rotation, while fusion-relevant temperatures lead to low resistivity. The question is whether plasma screening effectively protects the plasma core, and assessing its beneficial and detrimental effects on alpha-particle confinement.

## 2. Error Fields

The heat flux of alpha particles transported by the TF ripple forms 12 hotspots on the first wall. These hotspots are associated with deeply trapped alpha particles whose orbits remain localized near the outer midplane. The expected coil misalignments break the toroidal symmetry of the ripple field and concentrate the power fluxes. Figure 2 shows the heat loads arising from the TF ripple and error fields for a coil setup with outer limb at $R_{\text{out}} = 10.0\,\text{m}$.

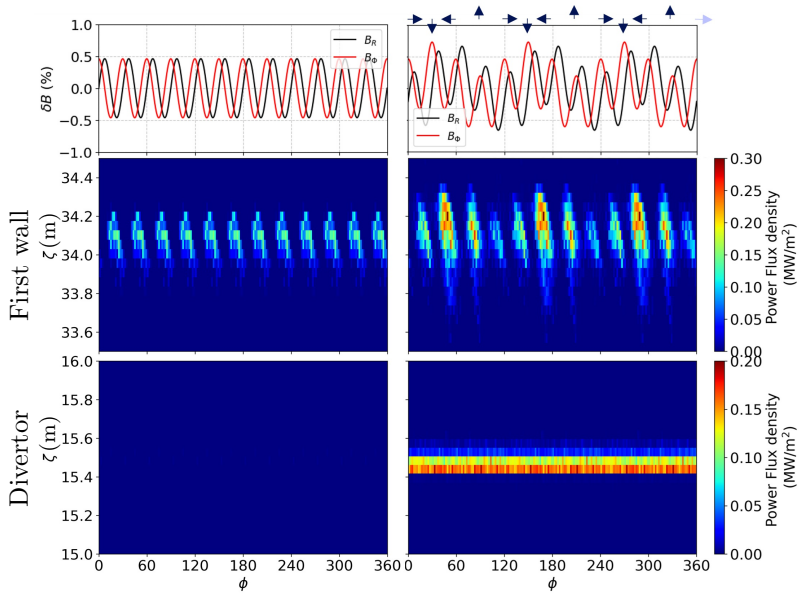


Figure 2: Magnetic field perturbation and associated power fluxes in TF ripple (left) and including error fields (right). The arrows above the figure indicate the direction of the offset, down/up for $-R/+R$ and left right for $-\phi/+\phi$.

The coordinate $\zeta$ in figure 2 denotes the poloidal distance along the first wall, starting at the inner midplane and increasing anti-clockwise. The outer midplane is located at $\zeta \approx 29.6\,\text{m}$.

Figures 3 present the total deposited power and peak of heat-flux density on the first wall and divertor for $R_{\text{out}} = 10.0\,\text{m}$ and $R_{\text{out}} = 10.5\,\text{m}$.

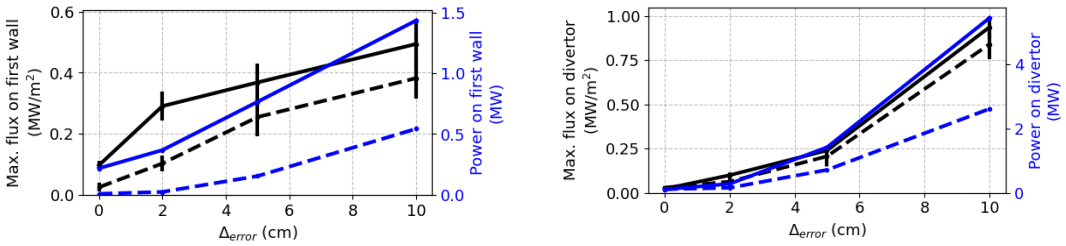


Figure 3: $R_{\text{out}} = 10\,\text{m}$ (solid) and $R_{\text{out}} = 10.5\,\text{m}$ (dashed) coil setup associated error field sensitivity scan for a range of $\Delta_{error}$ showing the maximum of heat flux and the overall power deposited in the first wall (left) and the divertor (right).

Small coil offsets of $\Delta_{\text{error}} = 2\,\text{cm}$ primarily redistribute the heat flux toroidally, concentrating power from the nominal 12 hotspots into a smaller number of locations, while leaving the total first-wall power largely unchanged. Larger offsets introduce additional transport channels, increasing alpha-particle losses to both the first wall and the divertor.

In the $R_{\text{out}} = 10.0\,\text{m}$ case, less than 2 cm of coil offset lead to heat flux exceeding $0.2\,\text{MWm}^{-2}$ on the first-wall. This configuration would therefore likely require robust error-field correction systems and/or local wall reinforcement. In contrast, for $R_{\text{out}} = 10.5\,\text{m}$, the same limit is reached only at offsets approaching 5 cm, larger than the expected maximum displacement of 3 cm. In this case, mitigation requirements may be modest or unnecessary.

## 3. Resonant Magnetic perturbation (RMP)

Resonant magnetic perturbations (RMPs) are an effective strategy for edge-localised mode (ELM) control. In STEP, two sets of 12 coils generate the applied perturbation, with current profiles optimised for ELM mitigation. The current profile also affects fast-ion confinement and the plasma response modifies the transport characteristics. Figure 4 shows an example of the applied current profile, the associated magnetic field and a set of cross section views comparing the three plasma response models.

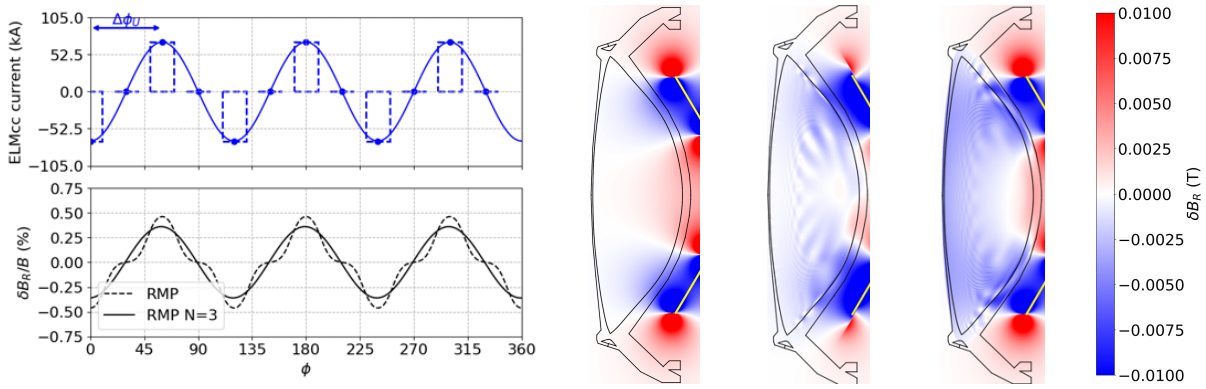


(a) Current profile (b) Vacuum (c) MARS-F (d) JOREK

Figure 4: a) Current profile and associated magnetic field. Comparison of magnetic field structures from vacuum (b), MARS-F (c), and JOREK (d) simulations.

In the vacuum case, only the externally applied field is considered, whereas MARS-F [4] includes the plasma response under ideal full-MHD, non-rotating plasma and JOREK [5] via resistive reduced-MHD, with slow-rotation assumptions. The two models shows qualitative agreement in the modification of the imposed perturbation.

The impact of these fields on alpha-particle confinement is shown in Figure 5, which illustrates the fraction of energy lost per characteristic orbit, based on the parameters $(v_\parallel/v^\star, \psi_N^\star)$, where the index $^\star$ indicates that the parameter is defined at the outer midplane, together with Poincaré maps illustrating field stochasticity. In the vacuum case, stochasticity extends to $\psi_N \approx 0.6$, affecting passing particles in the core, and leading to enhanced losses. MARS-F and JOREK reduces stochastic transport through plasma screening, while enhancing transport of trapped particles, especially near the trapped–passing boundary. The proportion of particles affected in the trapped–passing boundary is different in each model.

Table 1 list the maximum of power flux in two distinct coil current profile configurations and the three plasma response models. In the vacuum case, significant heat loads appear on the inner wall, reaching approximately $0.2\,\text{MWm}^{-2}$ due to passing particles drifting towards the low-field side. In contrast, plasma response strongly redistributes the heat flux, reducing first-wall peak loads to below $0.1\,\text{MWm}^{-2}$ but increasing divertor localisation in some toroidal regions, particularly for $\Delta\phi_{L,U} = 60°$. The low rotation and finite resistivity model in JOREK predicts generally weaker first-wall heat loads than the ideal MHD static setup used in MARS-F, with values remaining below design limits.

| | Alpha power lost (MW) | | Peak heat flux Divertor ($\text{MW/m}^2$) | | Peak heat flux First wall ($\text{MW/m}^2$) | |
|---|---|---|---|---|---|---|
| | $\Delta\phi_{L,U} = 0°$ | $\Delta\phi_{L,U} = 60°$ | $\Delta\phi_{L,U} = 0°$ | $\Delta\phi_{L,U} = 60°$ | $\Delta\phi_{L,U} = 0°$ | $\Delta\phi_{L,U} = 60°$ |
| Vacuum | 3.7 | 0.1 | 0.7 | 0.2 | 0.2 | $< 0.1$ |
| MARS-F | 0.6 | 4.1 | 0.2 | 0.7 | $< 0.1$ | 0.3 |
| JOREK | 1.9 | 1.1 | 0.4 | 0.3 | $< 0.1$ | $< 0.1$ |

Table 1: Overall power and peak of power flux density on each component in the vacuum case and plasma response case.

For $\Delta\phi_{L,U} = 0°$, the vacuum case shows the highest alpha power loss (3.7 MW), while MARS-F and JOREK predict reduced losses of 0.6 MW and 1.9 MW, respectively. For $\Delta\phi_{L,U} = 60°$, the loss ordering reverses, with

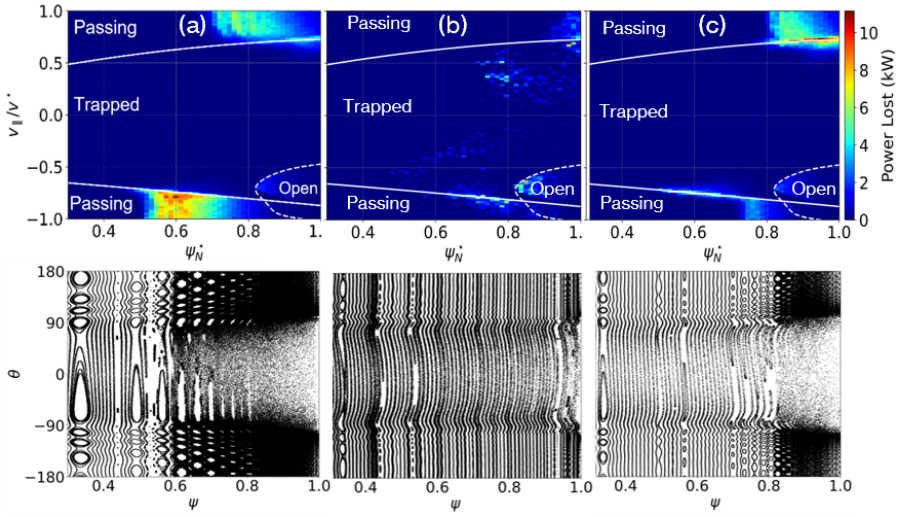


Figure 5: Loss region in the fast ion phase space of power lost in the (a) Vacuum (b) MARS-F and (c) JOREK.

MARS-F predicting the largest losses (4.1 MW), followed by JOREK (1.1 MW), while the vacuum case becomes negligible in comparison.

The results confirm that the plasma response plays a key role in redistributing fast-ion losses, and the heat loads are negligible in most cases. The exception of increased maximum heat flux in the RMP case with an ideal MHD plasma response $\Delta\phi_{L,U} = 60°$ is currently under investigation and is likely due to coupling with a core mode. Despite these differences, the enhanced heat flux is only slightly above the conservative maximum. Repeating the simulation with a realistic shape of the PFCs will help verify whether any reinforcement is needed.

## 4. Conclusion

The STEP static 3D field configuration does not significantly affect alpha-heating performance. In most cases, peak heat loads remain within design limits. The only exceptions require repeating the simulation with realistic 3D-shaped plasma-facing component (PFC) geometries, which may indicate the need for local first-wall reinforcement.

With an appropriately sized toroidal field (TF) coil, error fields are not expected to be a limiting concern.

The plasma response can either reduce or enhance the alpha particle transport. Results from JOREK and MARS-F show partial agreement, with discrepancies primarily arising from differences in modelling assumptions and equilibrium setups. A more detailed comparison is currently in progress to isolate the sources of these differences. Despite the variations, both approaches indicate that peak first-wall heat flux remains at low levels.

## 5. Acknowledgements

This work has been funded by STEP, a major technology and infrastructure programme led by UK Fusion Energy, which aims to deliver the UK's prototype fusion powerplant and a path to the commercial viability of fusion.

## References

[1] K. McClements et al. *Plasma Physics Controlled Fusion* **57** 075003 (2015).

[2] A. Prokopyszyn et al. *Nuclear Fusion* **65** 086039 (2026).

[3] K. Särkimäki et al. *Nuclear Fusion* **58** 076021 (2018).

[4] Y. Q. Liu et al. *Physics of Plasmas* **7** 3681 (2000).

[5] M Hoelzl et al. *Journal of Physics: Conference Series* **401** 012010 (2012).